NIH Public Access
Author Manuscript
Int J Radiat Oncol Biol Phys. Author manuscript; available in PMC 2009 July 15.

Published in final edited form as:
Int J Radiat Oncol Biol Phys. 2008 July 15; 71(4): 1236–1244.

Development of gene expression signatures for practical radiation biodosimetry

Sunirmal Paul, Ph.D. and **Sally A. Amundson, Sc.D.**
Center for Radiological Research, Columbia University Medical Center, New York, NY 10032, USA

Abstract

Purpose—In a large-scale radiological emergency, estimates of exposure doses and radiation injury would be required for individuals without physical dosimeters. Current methods are inadequate for the task, so we are developing gene expression profiles for radiation biodosimetry. This approach could provide both an estimate of physical radiation dose and an indication of the extent of individual injury or future risk.

Methods and Materials—We used whole genome microarray expression profiling as a discovery platform to identify genes with the potential to predict radiation dose across an exposure range relevant for medical decision-making in a radiological emergency. Human peripheral blood from ten healthy donors was irradiated *ex vivo*, and global gene expression was measured six and 24 hours after exposure.

Results—A 74-gene signature was identified that distinguishes between four radiation doses (0.5, 2, 5 and 8 Gy) and controls. Over a third of these genes are regulated by TP53. A Nearest Centroid classifier using these same 74 genes correctly predicted 98% of samples taken either six or 24 hours after treatment as unexposed, exposed to 0.5 Gy, to 2 Gy, or to 5 Gy and above. Expression patterns of five genes (*CDKN1A*, *FDXR*, *SESN1*, *BBC3* and *PHPT1*) from this signature were also confirmed by real-time PCR.

Conclusions—The ability of a single gene set to predict radiation dose throughout a window of time without need for individual pre-exposure controls represents an important advance in the development of gene expression for biodosimetry.

Keywords

ionizing radiation; biodosimetry; p53; microarray; peripheral blood lymphocytes

Introduction

In a climate of increasing concern about the possibility of a terrorist attack using radiological or nuclear devices, the Office of Science and Technology Policy and the Homeland Security Council established an interagency working group to assess and prioritize needs for a response to such a threat. The establishment of new biomarkers and approaches to biodosimetry was

Corresponding Author: Sally A. Amundson, Center for Radiological Research, Columbia University Medical Center, 630 W. 168th St. VC11-215, New York, NY 10032, Tel. 212-342-0965, Fax 212-305-3229, Email: saa2108@columbia.edu.

Conflicts of interest notification: Neither of the authors of this manuscript have any conflicts of interest associated with this work.

Publisher's Disclaimer: This is a PDF file of an unedited manuscript that has been accepted for publication. As a service to our customers we are providing this early version of the manuscript. The manuscript will undergo copyediting, typesetting, and review of the resulting proof before it is published in its final citable form. Please note that during the production process errors may be discovered which could affect the content, and all legal disclaimers that apply to the journal pertain.

NIH-PA Author Manuscript
NIH-PA Author Manuscript
NIH-PA Author Manuscript

NIH-PA Author Manuscript

NIH-PA Author Manuscript

NIH-PA Author Manuscript

identified as a high-priority need (1). Even a relatively small radiological dispersal device (a so-called "dirty bomb") set off in a large city could have the potential to cause worry and panic to tens or hundreds of thousands of people. An improvised nuclear device, on the other hand, would additionally result in a major health emergency, both in terms of immediate injury and later risks of cancer and other diseases. In the absence of physical dosimeters, such an event would require a rapid means to assess radiation exposure using biological markers, both to reassure the "worried well," and to assign those with significant exposure to appropriate medical care, ideally within the first 2-3 days. Biological dosimetry is expected to become increasingly important as ongoing research initiatives result in availibility of new mitigating agents and other treatments for radiation exposure (2). Although early administration of such countermeasures is desired in order to provide the best effect, risks of associated toxicities will likely counterindicate administration to entire populations in the absence of exposure information. Biologically based measurements could also be of value in follow-up epidemeological studies, where they could be correlated to individual disease outcomes and variations in radiation response.

While the dicentric assay is the reigning gold-standard for radiation biodosimetry, without automation it is not feasible to implement on the scale that would be necessary in a mass casualty situation (3,4). Even with full automation, scoring dicentrics requires stimulation of cell division, thus requiring a minimum of about three days before results could be available. Since gene expression does not require cell division, Lab-on-a-chip approaches to analysis (5) could provide results in the field within several hours of drawing blood.

We have previously suggested the development of gene expression profiles in peripheral blood lymphocytes (PBL) as an alternate approach to radiation biodosimetry (6-8). Exposure of human cells to environmental stresses, including ionizing radiation, is known to activate multiple signal transduction pathways, and rapidly results in complex patterns of gene expression change. Both basal gene expression patterns (9) and responses to radiation (10) have been correlated to radiation sensitivity in cell lines. Expression of specific genes can be both dose- and stress-dependent (11), and altered gene expression may persist for many days after exposure (12), providing an opportunity for dosimetric assessment. Circulating lymphocytes are both sensitive to early radiation injury and highly responsive in terms of induced gene expression changes (6,8,13). As they are also relatively easily biopsied, unstimulated PBL provide an ideal model for development of a gene expression biodosimeter for radiation exposure. Along with the coordinated development of rapid automated gene expression assays, such as a self-contained "lab-on-a-chip" device, this approach could provide an attractive high-throughput alternative to current biodosimetry assays.

In our initial studies, we *ex vivo* irradiated PBL separated from whole blood, and used microarray analysis to identify 55 radiation responsive genes 24 hours after irradiation. We also demonstrated a linear dose-response for induction of genes including *DDB2, CDKN1A* and *XPC* between 0.2 and 2 Gy at both 24 and 48 hours after irradiation of quiescent lymphocytes (6). These radiation responses were not enhanced in cells stimulated to divide by phytohemagglutinin. Similar patterns of gene response occurred *in vivo* in patients undergoing total body irradiation (8), along with some additional pathways that did not appear to respond in the *ex vivo* studies. Subsequent studies using microarray (14,15) or real-time PCR (16,17) approaches continue to develop the concept of gene expression in PBL for radiation biodosimetry.

In the present study, we have used whole genome microarrays to systematically identify genes potentially useful for biodosimetry through a broader dose range that would be relevant for radiological triage. This gene expression signature was then used to build a Nearest Centroid classifier that correctly predicted exposure range in 98% of the samples. Quiescent whole blood

NIH-PA Author Manuscript

NIH-PA Author Manuscript

NIH-PA Author Manuscript

was irradiated *ex vivo*, and RNA was profiled at 6 and 24 hours after exposure, representing a window of time that would be practical for medical decision-making in a mass-casualty situation. In order to best discriminate between un-irradiated and irradiated samples, and between different doses, we have employed the Agilent one-color hybridization approach that avoids analysis of individual ratios of gene response, but which has been shown to yield equivalent quality data to the two-color ratio technique (18). This approach enables direct comparison of variability among un-irradiated individuals, as well as providing radiation profiles independent of pre-exposure controls. It contrasts with the majority of studies of gene expression response to radiation, which have tended to examine ratios of expression in irradiated samples compared to unirradiated controls. This is a critical consideration in developing biodosimetry, as individual pre-exposure baselines would not be available for comparison in a situation where mass radiological triage was needed.

Methods and Materials

Irradiation and culture

Peripheral blood from healthy volunteers was obtained with informed consent from all subjects and was drawn into 0.105 M sodium citrate vacutainer tubes (Becton Dickinson and Company, Franklin Lakes, NJ). A total of 5 male and 5 female donors with ages ranging from 20 to 53 years (median age 36) participated in the study. The blood was divided into 3 ml aliquots and exposed at a rate of 0.82 Gy per minute to 0, 0.5, 2, 5 or 8 Gy γ-rays using a Gammacell-40 ^{137}Cs irradiator (AECL, Ontario, Canada). After irradiation, blood samples were diluted 1:1 with RPMI 1640 medium (Mediatech Inc., Herndon, VA) supplemented with 10% heat-inactivated fetal bovine serum (HyClone, Logan, UT) as described (19) and were incubated for 6 (2 male and 3 female donors) or 24 (3 male and 2 female donors) hours at 37 °C in a humidified incubator with 5% CO_2. All experiments involving human subjects were approved by the Columbia University Medical Center Institutional Review Board IRB #3, and were conducted according to the principles expressed in the Declaration of Helsinki.

Purification of RNA

RNA was prepared using the Versagene™ Blood RNA Purification kit (Gentra Systems, Minneapolis, MN) following the manufacturer's recommendations. This protocol differentially lyses red and white blood cells in whole blood. The red blood cells are lysed first and the nucleic acids released are washed away prior to lysis of the white blood cells for purification of RNA and on-column DNase treatment. This procedure depletes globin mRNA, but relatively high levels were still detected by semi-quantitative RT-PCR with β-globin specific primers (data not shown). As high amounts of globin message may affect detection of gene expression signatures derived from whole blood (20), globin mRNA was further reduced using GLOBINclear™ (Ambion Inc., Austin, TX) to specifically remove both α- and β- globin. RNA was quantified using a NanoDrop-1000 spectrophotometer and quality was monitored with the Agilent 2100 Bioanalyzer (Agilent Technologies, Santa Clara, CA). All RNA samples had RNA integrity numbers (21) between 7 and 10 (mean 8.3), 28S/18S ratios 0.6-2.5 (mean 1.3) and 260/280 absorbance ratios of 2.0-2.2 (mean 2.07).

Quantitative Real-Time PCR

500 ng total RNA was reverse transcribed to cDNA using the High-Capacity cDNA Archive Kit (Applied Biosystems, Foster City, CA) according to the manufacturer's instructions. Gene-specific primers and probes (Supplemental Table 1) were designed with the aid of Applied Biosystems' Primer Express® software and GeneScript Corporation's online TaqMan Primer Design software, sequences for *CDKN1A* were the same as used previously (8). Probes were synthesized by Operon Biotech, Inc. (Huntsville, AL) with 6-carboxyfluorescein (FAM) at the 5′ end and BHQ1quencer at the 3′ end. Standard curves were generated to optimize the amount

NIH-PA Author Manuscript

NIH-PA Author Manuscript

NIH-PA Author Manuscript

of input cDNA for measurement of each gene (5 or 10 ng). Real-time PCR reactions were performed with the ABI 7300 Real Time PCR System using Universal PCR Master Mix from ABI and following manufacturer's recommendations. All samples were run in duplicate and repeated a second time on a different day for each gene. Relative fold-inductions were calculated by the $\Delta\Delta C_T$ method as previously used (8) with averaged relative levels of *ACTB* and *GAPDH* used for normalization.

Microarray Hybridization and Data Extraction

Cyanine-3 (Cy3) labeled cRNA was prepared from 0.5 μg RNA using the One-Color Low RNA Input Linear Amplification PLUS kit (Agilent) according to the manufacturer's instructions, followed by RNAeasy column purification (QIAGEN, Valencia, CA). Dye incorporation and cRNA yield were checked with the NanoDrop ND-1000 Spectrophotometer. 1.5 μg of cRNA with incorporation of >10 pmol Cy3 per μg cRNA was fragmented and hybridized to Agilent Whole Human Genome Oligo Microarrays (G4112A) using the Gene Expression Hybridization Kit as recommended by Agilent. After hybridization with rotation for 17 hours at 65°C, microarrays were washed 1 minute at room temperature with GE Wash Buffer 1 (Agilent) and 1 minute with 37°C GE Wash buffer 2 (Agilent). Slides were scanned immediately using the Agilent DNA Microarray Scanner (G2404B). The images were analyzed with Feature Extraction Software 9.1 (Agilent) using default parameters for background correction, and flagging of non-uniform features.

Analyses in BRB ArrayTools

Background corrected hybridization intensities were imported into BRB-ArrayTools, Version 3.5 (22) log2-transformed and median normalized. Non-uniform outliers or features not significantly above background intensity in 25% or more of the hybridizations were filtered out, leaving 21939 features. A further filter requiring a minimum 1.5-fold change in at least 10% of the hybridizations was then applied yielding a final set of 17313 features that were used in subsequent analyses. The microarray data is available through the GEO database using accession number GSE8917.

Class comparisons were conducted using BRB-ArrayTools to identify genes that were differentially expressed between the five radiation doses using a random-variance F-test, an improvement over the standard F-test that permits sharing information among genes about within-class variation without assuming that all genes have the same variance (23). The test compares the differences in mean log-intensities between classes relative to the expected variation in mean differences computed from the independent samples. Genes with p-values less than 0.001 were considered statistically significant. The false discovery rate (FDR) was also estimated for each gene using the method of Benjamini and Hochberg (24), to control for false positives. Data was analyzed for the two times separately, and again for all data together without consideration of the time variable.

Multidimensional scaling (MDS) was performed in BRB-ArrayTools in order to create a low dimensional graphical representation of the high-dimensional data comprising the identified gene expression signature. The Euclidian distance metric was used to compute a distance matrix and the principal components of the gene expression signature. The first three principal components were used as axes to generate a plot. A global test for clustering based on the first three principal components was used to test the null hypothesis that all the expression profiles were drawn from a single multivariate Gaussian distribution (one cluster). The distribution of nearest neighbor distances for the actual data were compared with Gaussian distributions of nearest neighbor distances generated by 10,000 random permutations of the data (25).

NIH-PA Author Manuscript

NIH-PA Author Manuscript

NIH-PA Author Manuscript

Class Prediction by the Nearest Centroid method was performed in BRB-ArrayTools using log-intensity values median-centered by gene. The centroid of a class (all samples of a given dose) is a vector containing the means of log-intensities of all samples in the class. The centroid vectors have a component for each gene in the signature. Centroids for each class are determined, and the distance of the expression profile for each test sample to the centroid of each class is measured. Each sample is then predicted to belong to the class corresponding to the nearest centroid. Leave-one-out cross-validation was performed, in which one sample is omitted from the model, and its class is predicted based on proximity to the centroids of the other samples. The process is repeated independently for each sample. The sensitivity of prediction for each class (N) was calculated as (number of Class N samples predicted to belong to Class N)/(total number of class N samples). Specificity was calculated as (number of non-N samples predicted as non-N)/(total number of non-N samples). Permutation p-values were also calculated for the cross-validated misclassification error rate by randomly permutating the class labels for all samples, and repeating the entire cross-validation process. The p-values represent the proportion of 10,000 random permutations that produced a cross-validated misclassification rate as low as that obtained with the actual class labels.

Results

Reproducibility of RNA expression responses

In our initial study of radiation-induced gene expression in human lymphocytes, we monitored responses of several genes up to 72 hours after exposure to doses between 0.1 and 2 Gy γ-rays (6). In that study we separated the mononuclear cells and irradiated them in culture medium rather than irradiating freshly drawn whole blood as in the present study. Expression of individual genes was also determined using a serial dilution quantitative hybridization technique rather than by quantitative real-time PCR (qRT-PCR), which was used in the present study. We used one of the genes from our initial study, *CDKN1A*, to compare the two experimental approaches. At the two doses common to both sets of experiments, the two approaches yielded nearly identical *CDKN1A* expression ratios at both six and 24 hours after exposure (Fig. 1). It should also be noted that the two experiments, performed seven years apart, represent different donors from different populations. This evidence that gene expression responses to ionizing radiation are relatively robust both to changes in experimental protocols and across donors suggests that gene expression signatures are likely to be translatable from discovery platforms to developing “fieldable” assay platforms more suitable for practical biodosimetry or clinical testing.

Microarray Experiments

Global gene expression in human blood was measured at six and 24 hours after exposure to doses of 0, 0.5, 2, 5 and 8 Gy γ-rays. Five independent experiments were performed at each time using different donors for each experiment and time-point. Agilent whole genome microarrays were hybridized using the Agilent one-color workflow in order to identify genes that could distinguish radiation dose from individual samples without the use of pre-exposure control ratios. This aspect of the analysis is very important for ultimate translation to a radiation triage situation, where pre-exposure controls for each individual would not be available. Filtering for quality and minimum change gave a set of 17313 features that were used in subsequent analyses.

Genes distinguishing between radiation doses

We first used the Class Comparison feature of BRB-ArrayTools to identify genes with different expression levels after exposure to the five doses of radiation when measured at 6 hours after treatment. In order to compare gene expression between more than two groups, the comparison was based on an F-test rather than the t-test commonly used for comparison of two groups. Six

NIH-PA Author Manuscript

NIH-PA Author Manuscript

NIH-PA Author Manuscript

hours after irradiation, 339 genes were found to be differentially expressed ($p<0.001$) at the five dose levels (Supplemental Table 2. Of these genes, 338 had a FDR <5%. At 24 hours after irradiation, 139 genes were identified as differentially expressed ($p<0.001$), 101 of which had a FDR <5% (Supplemental Table 3). The intersection of the six- and 24-hour gene sets yielded 76 sequences representing 69 unique genes that responded significantly at both times (Table 1 and Fig. 2).

Since a substantial number of genes were common between the two times assayed, we next performed a class comparison of the five doses pooling all the data from the two times. This analysis identified 233 differentially expressed genes ($p<0.001$), with 201 genes at FDR <5% (Supplemental Table 4). Of the 76 sequences distinguishing dose in both the 6 and 24 hours post treatment data sets when the two times were analyzed separately, 74 (97%) were also found in the 201 gene set distinguishing dose across all samples in the pooled data irrespective of time (Table 1). Multidimensional scaling (MDS) was used to visualize the similarities between gene expression levels of this 74-gene consensus signature for all samples (Fig. 3). MDS is a visualization tool that allows graphical representation of high-dimensional data in two or three dimensions, while preserving all pair-wise similarities between samples. The first three principal components of the gene expression data are used as axes and a plot is created where each sample is represented by a single point, and the distance between any two points reflects the overall similarity of the expression levels of all 74 genes in the signature. Clustering by dose was significant ($p<0.0001$; global test for clustering (25)), indicating a low probability that all samples came from a single homogeneous cluster.

Prediction of radiation dose to individual samples

We next tested the ability of the 74-gene signature to predict the exposure dose of individual samples. Expression information for the 74 genes was used to build a Nearest Centroid Classifier with leave-one-out cross validation. The permutation p-value of the cross-validated misclassification error rate was $p<0.0001$. Using all five dose categories, we obtained 78% correct classification, with five 5 Gy and five 8 Gy samples incorrectly predicted to belong respectively to the 8 Gy and 5 Gy classes. One 2 Gy sample was also predicted to have received 5 Gy. Thus, the worst performance of the classifier was in distinguishing between 5 and 8 Gy samples, consistent with the visual representation of the data in Fig. 3. Since classification into four dose ranges would still be valuable for medical treatment, we next built a Nearest Centroid Classifier using leave-one-out cross validation to predict samples as belonging to the unexposed, 0.5 Gy, 2 Gy or 5-8 Gy categories. 98% of the samples were now classified correctly ($p<0.0001$), with one false positive in the highest dose category. The sensitivity and specificity of these classifiers are summarized in Table 2.

Dose responses of individual genes

To confirm the microarray results, we measured the radiation dose-response of five genes (*CDKN1A*, *FDXR*, *SESN1*, *BBC3* and *PHPT1*) from the gene set in Fig. 2. qRT-PCR was performed on all samples and plotted as average response ratios (Fig. 4). There was no significant difference between radiation responses of PBL from male or female donors for any of the genes tested ($0.54\leq p\leq 0.95$). All genes tested responded with the same general pattern as that seen on the microarrays, showing increasing expression with increasing dose, but decreased slope of the dose-response curve above 2 Gy. This flattening dose-response curve is consistent with our previous observation of flattening of the *CDKN1A* radiation dose-response at around 2.5 Gy in a human myeloid cell line (26). The observed non-linearity of gene expression responses is also consistent with the lessening of separation between doses at the high end of the range seen by MDS (Fig. 3), and the relatively poor performance of the classifier in distinguishing between 5 and 8 Gy (Table 2).

NIH-PA Author Manuscript

NIH-PA Author Manuscript

NIH-PA Author Manuscript

Discussion

The ability of a single set of genes to predict radiation dose at both six and 24 hours after exposure without the need for a pre-exposure sample is an important advance for gene expression biodosimetry. It suggests that gene expression signatures are likely to be informative across a range of doses and throughout a window of time, so that separate signatures for very narrow time or dose intervals should not be needed. A striking dose-response trend that is consistent at both times is also evident when expression of our 74-gene set is visualized by MDS (Fig. 3). The separation by exposure dose is clearest between the lower doses, with some overlap evident between the highest doses of 5 and 8 Gy. Although prediction of 5 versus 8 Gy samples was relatively poor, the 74-gene signature was able to predict exposure in the 5 to 8 Gy range for 100% of the samples, with only one false positive prediction of a 2 Gy sample. Indication of exposure in the 5-8 Gy range would call for rapid medical intervention and further testing. As doses rise above this range, any biodosimetric method based on lymphocytes, including the gold-standard cytogenetic methods, will be of decreasing utility, since lymphocytes will be rapidly lost from circulation. Prediction of unexposed samples and the lower exposure doses was also very good, with only one false classification of a 2 Gy sample, as mentioned above.

An effect of time since irradiation is also evident in the 74-gene signature (Fig. 3). At least some of this difference may be due to time in culture, however, as a similar separation between time points is seen at all doses, including the un-irradiated controls. Effects of time in culture on some individual genes can also be seen among the control samples in the Fig. 2 heat map. In a previous study of long-term primary human lymphocyte cultures assayed between 7 and 55 days, substantial gene expression responses were also attributable to time in culture (12). The combined effects of time in culture, time since exposure, and inter-individual variation do not prevent the classification of samples by dose, however.

We compared our current findings with our previous analysis of *in vivo* irradiation in patients undergoing total body irradiation (TBI) prior to transplant (8). Due to the requirements for much larger amounts of RNA for microarray analysis at the time of that study, only one of eight TBI patients could be assayed by microarray. The majority of the genes in our current 74 gene radiation profile set were not represented on that earlier microarray, but of the 20 that were, 8 (40%) were responsive to *in vivo* irradiation (Table 1). In a more recent whole genome study using TBI patients, Dressman *et al.* (15) reported 18 human genes that predicted radiation exposure, 13 of which (72%) were also included in our 74-gene consensus set (Table 1). The same study also reported a larger set of genes defining exposure to individual doses in mice irradiated *in vivo*. We identified human homologs of 106 of these genes, but only four were present in our 74-gene human consensus set. As the mouse genes were only measured at six hours post-irradiation, we also compared them against our set of 338 genes distinguishing all doses at six hours after exposure, finding eight genes in common. This low correspondence between mouse and human responses reflects major differences between *in vivo* radiation gene expression responses in mice and humans also reported by Dressman *et al.* (15).

Our finding of a large set of genes with dosimetric potential across the whole range of doses studied contrasts with the findings of Dressman *et al.* (15), who did not reported pronounced continuous dose-response patterns among the genes responding in mice. In fact, the majority of the genes in their profiles were informative only for a single dose, with many either responding only at one dose, or showing increased expression at one dose and decreased expression at another. This more complex dose-response behavior may be specific to mice, or may result from the additional interplay of signaling *in vivo*, and practical application will require determination of the precise range of doses and times where a human signature is informative. If our more broadly informative signatures can be translated to the human *in*

NIH-PA Author Manuscript

NIH-PA Author Manuscript

NIH-PA Author Manuscript

vivo situation, the approach may prove even more useful for emergency radiological triage than signatures derived from mice would predict.

Examination of our 74-gene consensus set reveals a strong contribution of the TP53 response to the overall potential dosimetric signature, with more than a third of the unique genes (24/67) having previous reports of regulation by TP53 (Table 1). The proportionately large contribution of TP53 response genes is consistent with the results of Dressman *et al.*, where 50% (9/18) of genes identified as radiation responsive in the TBI patients were also known TP53-regulated genes. This apparent dominance of the TP53 pathway in regulating the most robustly radiation responsive genes is a common finding of radiation gene expression studies in many model systems from cancer cell lines (27) to human peripheral blood (8) and lymphocyte subpopulations (13,28). Activation of TP53 is a common general response to many kinds of stress, but it can still produce agent-specific gene expression profiles (11,29). Nonetheless, the dominance of this common stress pathway in our radiation signatures underscores the need to determine the specificity of potential biomarkers before they can be usefully employed for biodosimetry.

Inter-individual variation is another important concern for the development of gene expression biomarkers. Within our set of ten donors, variations by radiation exposure dose were greater than the variations in expression between donors, allowing relatively accurate classification of samples by dose. A recent study of radiation induced gene expression in human PBL using real-time PCR reported minimal variance of baseline expression and consistent radiation responses of five genes among 20 healthy donors (17). Four of the five genes in that study were also in our 74-gene signature. The same study also concluded that responses of multiple genes, or ratios of responses, such as the *BAX:BCL2* expression ratio, were likely to provide better biodosimetry and be more robust to variation than single genes. This supports the likely usefulness of radiation dose prediction based on gene expression profiles.

Although further studies of inter-individual variation in larger populations including a broad range of ages, co-morbidities, ethnicities and lifestyles are still needed, the use of genomic responses also opens the possibility of exploiting specific inter-individual variation to make personal injury assessments integrating the sensitivity of an individual with information about the physical radiation dose. Such information would have additional value in long-term epidemiological studies following any large-scale radiological event. The study of potential correlations between gene expression and specific radiation injury or long-term outcomes like carcinogenesis should be a high priority in future studies, as such information would be useful not only in the event of a radiological incident, but also in clinical radiation oncology.

Gene expression signatures are looking increasingly attractive as potential biodosimeters for radiation exposure. However, further validation in terms of *in vivo* responses in cancer patients and animal models (including non-human primates), inter-individual variability and radiation specificity of the signatures is still needed. Other future areas for investigation also include the study of gene expression responses to partial body irradiation (30), responses to internal emitters, and the effects of age, co-morbidities, combined injuries, low dose-rate exposures, and different radiation qualities.

In order to make gene expression signatures practically useful for mass casualty screening, they will also need to be ported from the laboratory-based microarray platforms currently used for discovery and research to more high-throughput forward-deployable platforms. Approaches have been suggested based on qRT-PCR (16), or on nanotechnology “lab-on-a-chip” designs (5). We are collaborating in the development of inexpensive self-contained cartridges to take a blood sample and automatically perform a chemo-luminescence based gene expression assay. The reduced volumes required in such a miniaturized platform provide the

NIH-PA Author Manuscript

NIH-PA Author Manuscript

NIH-PA Author Manuscript

added benefit of dramatically reduced hybridization times, providing a convenient high-throughput assay that could pave the way for many practical applications of gene expression signatures in biodosimetry, biomonitoring, epidemiology and medical diagnostics.

Supplementary Material

Refer to Web version on PubMed Central for supplementary material.

Acknowledgements

We thank Drs. Michael Bittner, Frederic Zenhausern and David Brenner for helpful discussions and critical reading of the manuscript. Analyses were performed using BRB-ArrayTools developed by Dr. Richard Simon and Amy Peng Lam. This work was supported by the Center for High-Throughput Minimally-Invasive Radiation Biodosimetry (NIAID grant U19 AI067773) and by National Institutes of Health Grant CA 49062.

References

1. Pellmar TC, Rockwell S. Priority list of research areas for radiological nuclear threat countermeasures. Radiat Res 2005;163:115–123. [PubMed: 15606315]
2. Alexander GA, Swartz HM, Amundson SA, et al. BiodosEPR-2006 Meeting: Acute Dosimetry Consensus Committee Recommendations on Biodosimetry Applications in Events Involving Terrorist Uses of Radioactive Materials and Radiation Accidents. Radiat Meas 2007;42:972–996.
3. Amundson SA, Meltzer P, Trent J, et al. Biological indicators for the identification of radiation exposure in humans. Expert Review of Molecular Diagnostics 2001;1:89–97.
4. Blakely WF, Salter CA, Prasanna PG. Early-response biological dosimetry--recommended countermeasure enhancements for mass-casualty radiological incidents and terrorism. Health Phys 2005;89:494–504. [PubMed: 16217193]
5. Liu RH, Yang J, Lenigk R, et al. Self-contained, fully integrated biochip for sample preparation, polymerase chain reaction amplification, and DNA microarray detection. Anal Chem 2004;76:1824–1831. [PubMed: 15053639]
6. Amundson SA, Shahab S, Bittner M, et al. Identification of potential mRNA markers in peripheral blood lymphocytes for human exposure to ionizing radiation. Radiation Res 2000;154:342–346. [PubMed: 11012342]
7. Amundson SA, Bittner M, Meltzer P, et al. Induction of gene expression as a monitor of exposure to ionizing radiation. Radiat Res 2001;156:657–661. [PubMed: 11604088]
8. Amundson SA, Grace MB, McLeland CB, et al. Human in vivo radiation-induced biomarkers: gene expression changes in radiotherapy patients. Cancer Res 2004;64:6368–6371. [PubMed: 15374940]
9. Torres-Roca JF, Eschrich S, Zhao H, et al. Prediction of radiation sensitivity using a gene expression classifier. Cancer Res 2005;65:7169–7176. [PubMed: 16103067]
10. Amundson SA, Do KT, Vinikoor LC, et al. Integrating global gene expression and radiation survival parameters across the 60 cell lines of the National Cancer Institute Anticancer Drug Screen. Cancer Res 2008;68:415–424. [PubMed: 18199535]
11. Amundson SA, Do KT, Vinikoor L, et al. Stress-specific signatures: expression profiling of p53 wild-type and -null human cells. Oncogene 2005;24:4572–4579. [PubMed: 15824734]
12. Falt S, Holmberg K, Lambert B, Wennborg A. Long-term global gene expression patterns in irradiated human lymphocytes. Carcinogenesis 2003;24:1837–1845. [PubMed: 12951355]
13. Mori M, Benotmane MA, Vanhove D, et al. Effect of ionizing radiation on gene expression in CD4 + T lymphocytes and in Jurkat cells: unraveling novel pathways in radiation response. Cell Mol Life Sci 2004;61:1955–1964. [PubMed: 15341025]
14. Kang CM, Park KP, Song JE, et al. Possible biomarkers for ionizing radiation exposure in human peripheral blood lymphocytes. Radiat Res 2003;159:312–319. [PubMed: 12600233]
15. Dressman HK, Muramoto GG, Chao NJ, et al. Gene expression signatures that predict radiation exposure in mice and humans. PLoS Med 2007;4:e106. [PubMed: 17407386]

NIH-PA Author Manuscript

NIH-PA Author Manuscript

NIH-PA Author Manuscript

16. Grace MB, McLeland CB, Gagliardi SJ, et al. Development and assessment of a quantitative reverse transcription-PCR assay for simultaneous measurement of four amplicons. Clin Chem 2003;49:1467–1475. [PubMed: 12928227]
17. Grace MB, Blakely WF. Transcription of five p53- and Stat-3-inducible genes after ionizing radiation. Radiation Measurements 2007;42:1147–1151.
18. Patterson TA, Lobenhofer EK, Fulmer-Smentek SB, et al. Performance comparison of one-color and two-color platforms within the MicroArray Quality Control (MAQC) project. Nat Biotechnol 2006;24:1140–1150. [PubMed: 16964228]
19. Grace MB, McLeland CB, Blakely WF. Real-time quantitative RT-PCR assay of GADD45 gene expression changes as a biomarker for radiation biodosimetry. Int J Radiat Biol 2002;78:1011–1021. [PubMed: 12456288]
20. Feezor RJ, Baker HV, Mindrinos M, et al. Whole blood and leukocyte RNA isolation for gene expression analyses. Physiol Genomics 2004;19:247–254. [PubMed: 15548831]
21. Schroeder A, Mueller O, Stocker S, et al. The RIN: an RNA integrity number for assigning integrity values to RNA measurements. BMC Mol Biol 2006;7:3. [PubMed: 16448564]
22. Simon R, Lam A, Li MC, et al. Analysis of gene expression data using BRB-Array Tools. Cancer Informatics 2007;2:11–17.
23. Wright GW, Simon RM. A random variance model for detection of differential gene expression in small microarray experiments. Bioinformatics 2003;19:2448–2455. [PubMed: 14668230]
24. Benjamini Y, Hochberg Y. Controlling the False Discovery Rate: A Practical and Powerful Approach to Multiple Testing. J R Statist Soc B 1995;57:289–300.
25. McShane LM, Radmacher MD, Freidlin B, et al. Methods for assessing reproducibility of clustering patterns observed in analyses of microarray data. Bioinformatics 2002;18:1462–1469. [PubMed: 12424117]
26. Amundson SA, Do KT, Fornace AJ Jr. Induction of Stress Genes by Low Doses of Gamma Rays. Radiat Res 1999;152:225–231. [PubMed: 10453082]
27. Amundson SA, Bittner M, Chen YD, et al. cDNA microarray hybridization reveals complexity and heterogeneity of cellular genotoxic stress responses. Oncogene 1999;18:3666–3672. [PubMed: 10380890]
28. Mori M, Benotmane MA, Tirone I, et al. Transcriptional response to ionizing radiation in lymphocyte subsets. Cell Mol Life Sci 2005;62:1489–1501. [PubMed: 15971001]
29. Hammond EM, Mandell DJ, Salim A, et al. Genome-wide analysis of p53 under hypoxic conditions. Mol Cell Biol 2006;26:3492–3504. [PubMed: 16611991]
30. Lee HJ, Lee M, Kang CM, et al. Identification of possible candidate biomarkers for local or whole body radiation exposure in C57BL/6 mice. Int J Radiat Oncol Biol Phys 2007;69:1272–1281. [PubMed: 17967317]
31. Tanabe L, Scherf U, Smith LH, et al. MedMiner: an Internet text-mining tool for biomedical information, with application to gene expression profiling. Biotechniques 1999;27:1210–4. 1216–7. [PubMed: 10631500]

NIH-PA Author Manuscript

NIH-PA Author Manuscript

NIH-PA Author Manuscript

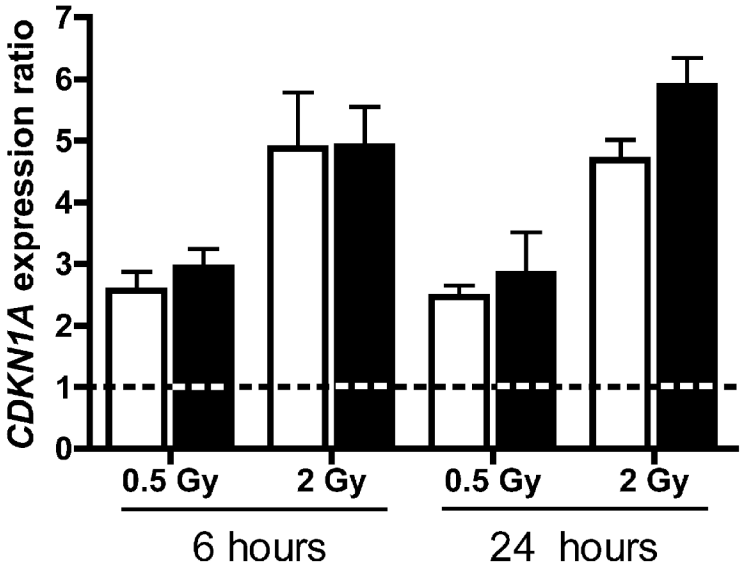

Figure 1.

Relative induction of *CDKN1A* by irradiation. White bars: quantitative hybridization data from (6)(n=4), black bars: current real-time PCR data (n=5). The measurements made using the two techniques are not significantly different from each other (p>0.05) at any dose or time. Dashed line indicates unirradiated control ratio.

NIH-PA Author Manuscript

NIH-PA Author Manuscript

NIH-PA Author Manuscript

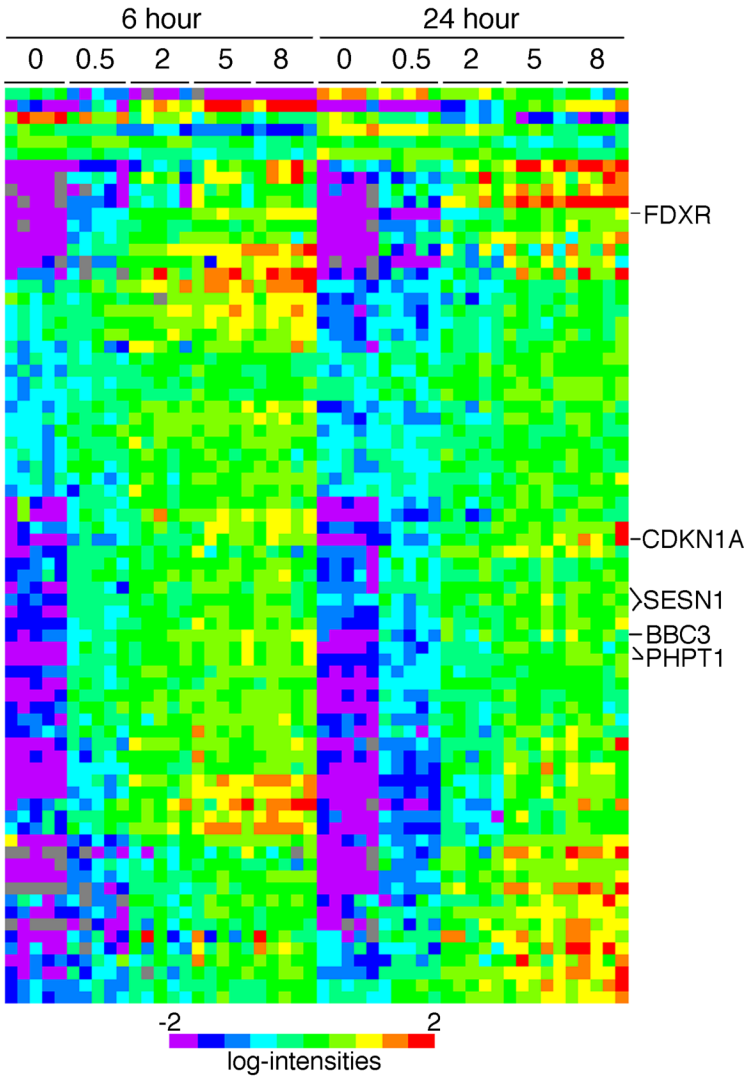

Figure 2.

Average linkage clustering of genes in the radiation consensus signature. Dose in Gray is shown across the top. Genes used for qRT-PCR are indicated along the right edge, and annotation of all genes in clustered order is presented in Table 1.

NIH-PA Author Manuscript

NIH-PA Author Manuscript

NIH-PA Author Manuscript

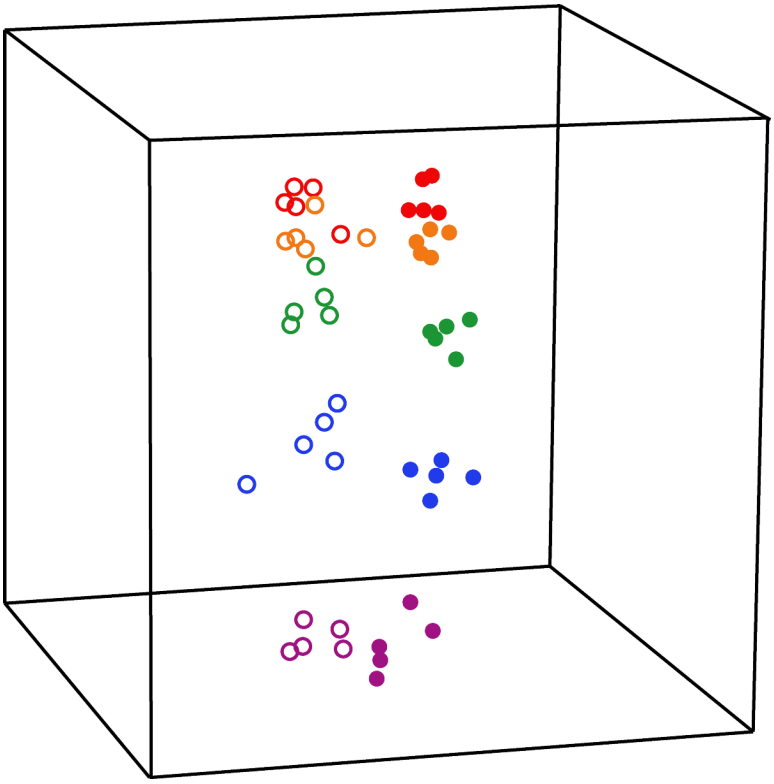

Figure 3.

The 74-gene consensus signature visualized by MDS. Open symbols: 6 hour samples, Filled symbols: 24 hour samples. Axes represent the first three principal components of gene expression. Each point represents the relative gene expression of all 74 array features for an individual sample. The distance between any two points reflects their overall similarity of expression levels of all 74 genes. The points are colored according to dose: 0 Gy (purple), 0.5 Gy (blue), 2 Gy (green), 5 Gy (orange) and 8 Gy (red).

NIH-PA Author Manuscript

NIH-PA Author Manuscript

NIH-PA Author Manuscript

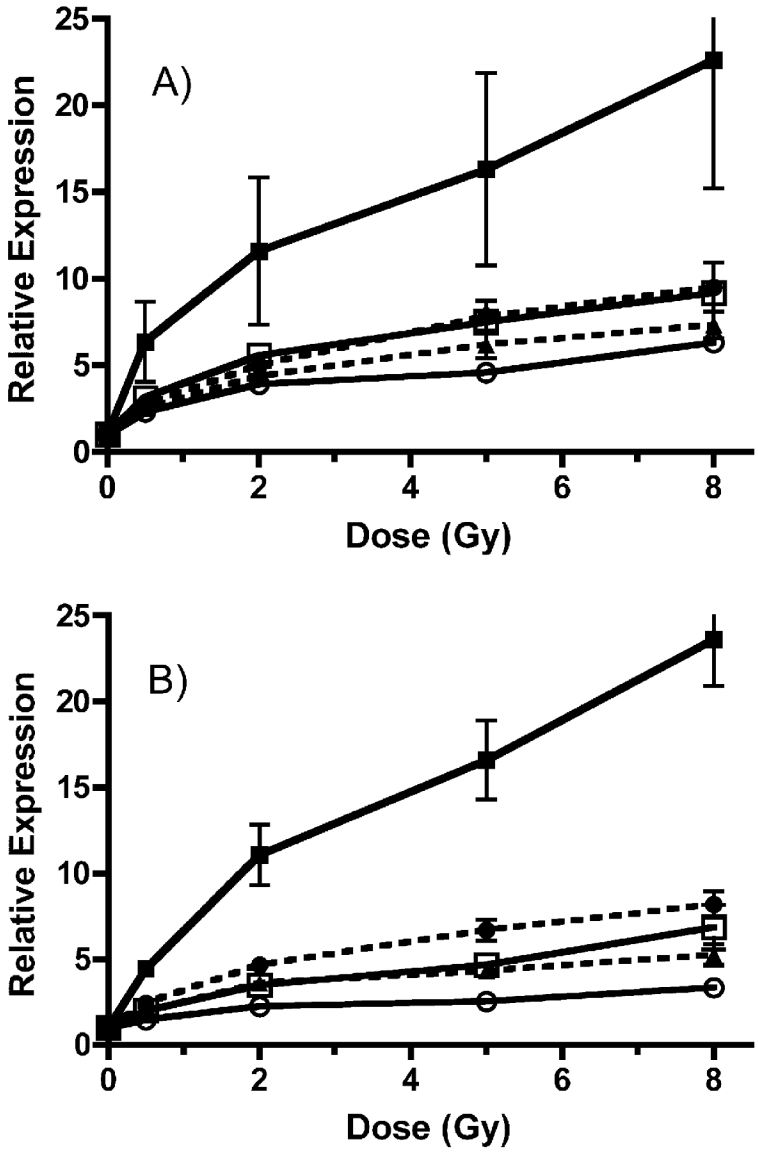

Figure 4.

Relative expression of FDXR (■), CDKN1A (●), PHPT1 (□), BBC3 (▲) and SESN1 (○) at A) 6 and B) 24 hours after irradiation as measured by qRT-PCR. Points are the mean of responses in 5 independent donors, error bars are standard errors.

NIH-PA Author Manuscript

NIH-PA Author Manuscript

NIH-PA Author Manuscript

Table 1

Consensus radiation dose-response signature

Agilent ID	Symbol	Accession	Description	PBL[1]	TBI[2]	TBI[3]	TP53[4]
39233*	GNG7	NM_052847	Guanine nucleotide binding protein (G protein), gamma 7	X	X		no
19925	VWCE	NM_152718	Von Willebrand factor C and EGF domains	X	X		no
19825	MYC	NM_002467	V-myc myelocytomatosis viral oncogene homolog (avian)	X	YES		YES
14330*	LY9	NM_002348	Lymphocyte antigen 9	X	no		no
25928	RASGRP2	NM_005825	RAS guanyl releasing protein 2 (calcium and DAG-regulated)	X	X		no
6537	TCF3	NM_003200	Transcription factor 3 (E2A immunoglobulin enhancer binding factors E12/E47)	no	no		no
34335	GDF15	NM_004864	Growth differentiation factor 15	X	X		YES
44034	N/A	N/A	N/A	X	X		no
12344	N/A	THC2439183	N/A	X	X		no
2293	APOBEC3H	NM_181773	Apolipoprotein B mRNA editing enzyme, catalytic polypeptide-like 3H	X	X		no
14295	FDXR	NM_024417	Ferredoxin reductase	X	X		YES
18124	ISG20L1	NM_022767	Interferon stimulated exonuclease gene 20kDa-like 1	X	X	YES	no
7064	ISG20L1	BE646426	Interferon stimulated exonuclease gene 20kDa-like 1	X	X	YES	no
19537	CD70	NM_001252	CD70 molecule	X	X		no
4401	TNFSF4	NM_003326	Tumor necrosis factor (ligand) superfamily, member 4	X	X		no
8181	MDM2	NM_006879	Mdm2, transformed 3T3 cell double minute 2, p53 binding protein (mouse)	X	X		YES
11507	IL21R	NM_181078	Interleukin 21 receptor	X	X		No
376	DRAM	NM_018370	Damage-regulated autophagy modulator	X	X		YES
19912	IER5	NM_016545	Immediate early response 5	X	X		no
18837	DRAM	NM_018370	Damage-regulated autophagy modulator	X	X		YES
9753	PLK3	NM_004073	Polo-like kinase 3 (Drosophila)	X	X		YES
18292	MGAT3	AF289562	Mannosyl (beta-1,4-)-glycoprotein beta-1,4-N-acetylglucosaminyltransferase	X	X		no
39508	ANKRA2	NM_023039	Ankyrin repeat, family A (RFXANK-like), 2	X	X		no
8281	BTG3	NM_006806	BTG family, member 3	X	no		no
4724	UROD	NM_000374	Uroporphyrinogen decarboxylase	no	YES		no
7164	TM7SF3	NM_016551	Transmembrane 7 superfamily member 3	X	X		no
1249	LOC284184	BC079831	Hypothetical LOC284184	X	no		no
20206	PPM1D	NM_003620	Protein phosphatase 1D magnesium-dependent, delta isoform	no	X		YES
23339	METTL7A	NM_014033	Methyltransferase like 7A	X	X		no
28072	ANXA4	NM_001153	Annexin A4	X	no		no
12866	PTP4A1	NM_003463	Protein tyrosine phosphatase type IVA, member 1	X	YES		no
4989	ARHGEF3	NM_019555	Rho guanine nucleotide exchange factor (GEF) 3	X	X		no
21293	C11orf24	NM_022338	Chromosome 11 open reading frame 24	X	X		no
29379	EI24	NM_004879	Etoposide induced 2.4 mRNA	X	X		YES
707	ASCC3	NM_006828	Activating signal cointegrator 1 complex subunit 3	X	X		no
868	TRIAP1	NM_016399	TP53 regulated inhibitor of apoptosis 1	X	X	YES	YES
12676	SLC7A6	NM_003983	Solute carrier family 7 (cationic amino acid transporter, y+ system), member 6	X	X		no
41848	CDKN1A	NM_000389	Cyclin-dependent kinase inhibitor 1A (p21, Cip1)	YES	YES	YES	YES
14030	CCNG1	NM_004060	Cyclin G1	YES	no		YES
41451	TRIM22	NM_006074	Tripartite motif-containing 22	YES	YES		YES
6936	TRIM22	NM_006074	Tripartite motif-containing 22	YES	YES		YES
10516	SESN1	NM_014454	Sestrin 1	X	X		YES
27376	DCP1B	NM_152640	DCP1 decapping enzyme homolog B (S. cerevisiae)	X	X		no
15163	SESN1	NM_014454	Sestrin 1	X	X		YES
16162	XPC	NM_004628	Xeroderma pigmentosum, complementation group C	no	YES	YES	YES
25481	BBC3	NM_014417	BCL2 binding component 3	X	X	YES	YES
12956	PHPT1	NM_014172	Phosphohistidine phosphatase 1	X	X	YES	no
30012	PHPT1	NM_014172	Phosphohistidine phosphatase 1	X	X	YES	no
20670	TNFRSF10B	NM_003842	Tumor necrosis factor receptor superfamily, member 10b	YES	no		YES
41670	BAX	NM_138764	BCL2-associated X protein	YES	no	YES	YES

NIH-PA Author Manuscript
NIH-PA Author Manuscript
NIH-PA Author Manuscript

Agilent ID	Symbol	Accession	Description	PBL[1]	TBI[2]	TBI[3]	TP53[4]
23613	RPS27L	NM_015920	Ribosomal protein S27-like	X	X	YES	YES
6680	BAX	NM_138765	BCL2-associated X protein	YES	no	YES	YES
30940	FBXO22	NM_012170	F-box protein 22	X	X		no
3595	TMEM30A	NM_018247	Transmembrane protein 30A	X	X	YES	no
41916	POLH	AK025631	Polymerase (DNA directed), eta	X	X		YES
8262	N/A	THC2340838	N/A	X	X		no
23059	GADD45A	NM_001924	Growth arrest and DNA-damage-inducible, alpha	no	YES		YES
20246	N/A	N/A	N/A	X	X		no
37206	PCNA	NM_002592	Proliferating cell nuclear antigen	YES	no		YES
11080	PLK2	NM_006622	Polo-like kinase 2 (Drosophila)	X	no		YES
10837	MGC5370	BC006795	Hypothetical protein MGC5370	X	X	YES	no
31861	N/A	THC2429167	N/A	X	X		no
8404	N/A	AK024898	CDNA: FLJ21245 fis, clone COL01184	X	X		no
13295	GLS2	NM_013267	Glutaminase 2 (liver, mitochondrial)	X	X		no
28993	N/A	AK056245	CDNA clone IMAGE:5261213	X	X		no
26429	DDB2	NM_000107	Damage-specific DNA binding protein 2, 48kDa	X	YES	YES	YES
33393	ASTN2	NM_014010	Astrotactin 2	X	X		no
4485	SLC4A11	NM_032034	Solute carrier family 4, sodium bicarbonate transporter-like, member 11	X	X		no
15190	ZMAT3	NM_022470	Zinc finger, matrin type 3	X	X	YES	YES
31519	C8orf38	AK074467	Chromosome 8 open reading frame 38	X	X		no
26679	ACTA2	NM_001613	Actin, alpha 2, smooth muscle, aorta	X	no	YES	no
28267	N/A	NM_032255	N/A	X	X		no
11881	SLC7A6	NM_003983	Solute carrier family 7 (cationic amino acid transporter, y+ system), member 6	X	X		no
40189	MAMDC4	NM_206920	MAM domain containing 4	X	X		no
10319	LIG1	NM_000234	Ligase I, DNA, ATP-dependent	YES	no		no
6722	ZNF337	NM_015655	Zinc finger protein 337	X	X		no

*not in time-independent dose signature - overlap of 6hr and 24hr signatures only.

[1]Data from (6); X= gene not present on array; no=no change in prior experiment; YES= same direction change in prior experiment.

[2]Data from (8); X= gene not present on array; no=no change in prior experiment; YES= same direction change in prior experiment.

[3]Data from (15); YES= reported in human radiation signature. (All genes presumed to be tested since whole genome platform was used.)

[4]Literature search for TP53 regulation of genes using MedMiner (31). No= no reported relationship found; YES= reported regulation by p53.

NIH-PA Author Manuscript

NIH-PA Author Manuscript

NIH-PA Author Manuscript

Table 2

Performance of the 74-gene classifier in predicting all five doses for samples assayed six and 24 hours after exposure (upper) or for predicting four dose ranges for the same samples (lower).

Dose (Gy)	Sensitivity	Specificity
	Five-dose prediction	
0	1	1
0.5	1	1
2	0.9	1
5	0.5	0.85
8	0.5	0.875
	Four-dose prediction	
0	1	1
0.5	1	1
2	0.9	1
5 or 8	1	0.967